UC Irvine
UC Irvine Previously Published Works

Title

Low temperature magnetism of Cd-doped Ce2RhIn8 heavy fermion antiferromagnet

Permalink

https://escholarship.org/uc/item/4893d0hm

Journal

Physica B Condensed Matter, 404(19)

ISSN

0921-4526

Authors

Adriano, C

Giles, C

Mendonça-Ferreira, L

et al.

Publication Date

2009-10-01

DOI

10.1016/j.physb.2009.07.030

Peer reviewed

Low temperature magnetism of Cd-doped Ce_2RhIn_8 heavy fermion antiferromagnet

C. Adriano [a,*], C. Giles [a], L. Mendonça-Ferreira [a], F. de Bergevin [b], C. Mazzoli [b], L. Paolasini [b], Z. Fisk [c], P.G. Pagliuso [a]

[a] Instituto de Física "Gleb Wataghin", UNICAMP, C. P. 6165, 13083-970 Campinas, SP, Brazil
[b] European Synchrotron Radiation Facility, Grenoble 38043, France
[c] University of California, Irvine, CA 92697-4574, USA

ABSTRACT

We report the low temperature magnetic properties of Cd-doped single crystals of Ce_2RhIn_8 grown from In-flux. Measurements of temperature-dependent magnetic susceptibility, heat capacity, electrical resistivity and X-ray magnetic scattering revealed that Cd-doping enhances the antiferromagnetic ordering temperature from $T_N = 2.8$ to $4.8\,K$ for crystals with nominal Cd-concentration of $\sim 20\%$. Similarly to the pure compound, Cd-doped Ce_2RhIn_8 presents just below T_N a commensurate antiferromagnetic structure with a propagation vector $\vec{\eta} = (\frac{1}{2}, \frac{1}{2}, 0)$. Comparisons between our results and the general effects of Cd-doping on the single layer related family $CeMIn_5$ (M = Co, Rh and Ir) will also be given.

© 2009 Elsevier B.V. All rights reserved.

1. Introduction

Superconducting heavy fermion materials belong to a class of correlated electron system where unconventional superconductivity (USC) is believed to be mediated by magnetic fluctuations [1,2]. The Ce_nMIn_{3n+2} (M = Co, Rh, Ir; $n = 1, 2$) series represents one of the most recently investigated family of this class of compounds. This family is a tetragonal variant of $CeIn_3$ because its structure can be viewed as being composed of n layers of $CeIn_3$ alternating with layers of MIn_2 [3,4].

The $n = 1$ member of the family, $CeMIn_5$ (1 – 1 – 5) was largely studied, and particularly, the investigations using many types of chemical substitutions gave rise to very rich phase diagrams that have allowed a deeper understanding of the interplay between antiferromagnetism (AFM) and USC and its relationship with dimensionality and crystal structures [5–10]. For example, the systematic substitution of Rh by Co and Ir in $CeRhIn_5$ have revealed a rich phase diagram with large regions of coexistence between antiferromagnetism and superconductivity [6,11]. In addition, studies concerning La-dilution on the Ce-sites in $CeRhIn_5$ described the evolution of the magnetic state as a function of La-doping (T_N decreases linearly with doping) [6,12]. Finally, more interesting and perturbative doping studies can be found in the

reports on in-block doping samples where the In atoms are replaced by Sn or Cd. The Sn substitution [8,10,13,14] in the $CeMIn_5$ (M = Co, Rh) materials has shown suppression of superconductivity in $CeCoIn_{5-x}Sn_x$ or antiferromagnetism in $CeRhIn_{5-x}Sn_x$, while the Cd substitution [9,15,16] in $CeCoIn_5$, drives the superconducting phase to an antiferromagnetic ground state. In particular, the nuclear magnetic resonance (NMR) studies [16] on Cd-doping $CeCoIn_5$ suggested that Cd-doping induces antiferromagnetic droplets inside the superconducting phase through an electronically tuning in Ce-sites which suppresses superconductivity locally. The scenario of local tuning seems also to be consistent with the existence of a zero resistance transition in the absence of bulk superconductivity in $CeRhIn_{5-x}Sn_x$ under pressure, where in this case, the Sn is believed to induce superconductivity locally [8]. However, the microscopic mechanisms of this electronic tuning of the ground state induced by Cd- and Sn-doping are unclear and there is no definite conclusion about how these dopants affect the single ion anisotropy and the relative magnetic interaction of the neighboring Ce^{3+} ions. To help answer these questions it would be very elucidative to extent these kind of doping studies to other members of the Ce_nMIn_{3n+2} (M = Co, Rh, Ir; $n = 1, 2$) series. An interesting candidate is the $n = 2$ member of the family with M = Rh, Ce_2RhIn_8 which is the by-layer relative of $CeRhIn_5$. Ce_2RhIn_8 orders in a commensurate AFM structure at $2.8\,K$ with the propagation vector $\vec{\eta} = (\frac{1}{2}, \frac{1}{2}, 0)$ [17] and it also becomes a superconductor under pressure. Despite of the interesting properties of the Ce_2MIn_8 (M = Rh, Ir, Co) family and

its interesting structural relationship to the $CeMIn_5$, the doping studies in the Ce_2MIn_8 were not investigated in great detail [18]. In this article, we present the low temperature physical properties and a preliminary study of the magnetic structure on a $Ce_2RhIn_{8-x}Cd_x$ sample with 20% Cd (nominal).

2. Experiment

Single crystalline samples of Ce_2RhIn_8 doped with Cd with a nominal concentration of 20% were grown from Indium flux [19,20]. The nominal concentration in this case is defined by the Cd/In ratio used in the growth. The tetragonal (P4/mmm) structure and unit cell parameters $a = 4.662(5)$ Å and $c = 12.24(5)$ Å was determined by X-ray powder diffraction. Within the studied range of concentration, no changes in the lattice parameters were found for the Cd-doped samples. Magnetization measurements were performed using a commercial superconducting quantum interference device (SQUID). Specific heat and electrical resistivity experiments were performed in a commercial physical properties measurement system (PPMS). The specific-heat set up uses a small mass calorimeter that employs a quasi-adiabatic thermal relaxation technique, while the electrical resistivity was measured using a low-frequency ac resistance bridge and four-contact configuration. The samples were previous screened and found to be free of surface contamination by residual In flux. For the X-ray magnetic scattering (XMRS) experiments, a selected crystal was extracted and prepared with polished $(0\,0\,l)$ flat surface, and sizes of approximately $4\,mm \times 3\,mm \times 2\,mm$. The preferred crystal growth direction of this compound is columnar along the $[0\,0\,1]$ direction and the $(0\,0\,1)$ facet is relatively large. The mosaic spread of the sample was found to be $< 0.04°$ by a rocking curve (θ scan) on a four-circle diffractometer. XRMS studies were performed at the ID-20 beamline at the European synchrotron radiation facility (ESRF). The ID-20 X-ray source is a linear undulator with a 32 mm period. The main optical components are a double Si(1 1 1) crystal monochromator with sagital focusing and two meridional focusing mirrors on either side of the monochromator. The sample was mounted on a cryostat (with a base temperature of 1.7 K using a Joule–Thomson stage), installed on a vertical HUBER four-circle diffractometer, with the a-axis parallel to the beam direction. This configuration allowed σ-polarized incident photons in the sample. During the measurements we have performed a polarization analysis, using LiF(2 2 0) crystal analyzer, appropriate for the energy of CeL_2 absorption edge.

3. Results and discussions

Fig. 1 shows the temperature dependence of the magnetic susceptibility measured for a magnetic field $H = 1\,kOe$ applied parallel $\chi_{||}$ (circles), and perpendicular $\chi_\perp$ (squares) to the c-axis for the pure (closed symbols) and Cd-doped (open symbols) Ce_2RhIn_8 single crystals. The dashed-dot line shows the inverse of the polycrystalline average of the magnetic susceptibility data taken as $\chi_{poly} = (\chi_{||} + 2\chi_\perp)/3$ for the doped sample. The inset in Fig. 1 shows in detail susceptibility as a function of the temperature in the low-T region. The results show antiferromagnetic order for $T_N < 4.8\,K$ with an easy axis along the c-axis, in agreement to what was found for the compounds in the In-based $R_mM_nIn_{3m+2n}$ (M = Co, Rh or Ir, $m = 1, 2$) series except for R = Gd [21–25]. The ratio $\chi_{||}/\chi_\perp$ taken at T_N is mainly determined by the tetragonal CEF and it reflects to some extent the CEF anisotropy. Fits from the inverse of $\chi_{poly}(T)$ for $T > 150\,K$ using a Curie–Weiss law yields an effective magnetic moment
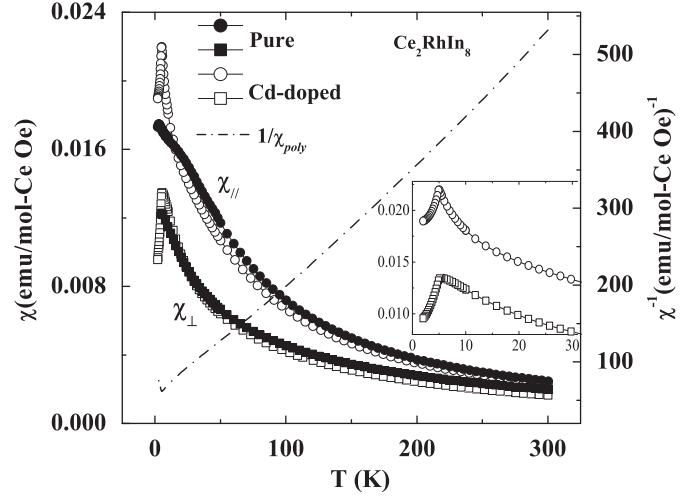
Fig. 1. Temperature dependence of the magnetic susceptibility for pure (close symbols) and Cd-doped (open symbols) Ce_2RhIn_8, for field $H = 1\,kOe$ applied parallel $\chi_{||}$ (circles) and perpendicular $\chi_\perp$ (squares) to the c-axis. The temperature dependence of the susceptibility inverse of the polycrystalline average is represented in the right axis (dashed-dot line). The inset shows the detailed Cd-doped susceptibility for low temperatures.

$\mu_{eff} = 2.2(1)\mu_B$ and a paramagnetic Curie–Weiss temperature $\theta_p = -10(1)\,K$.

The temperature dependence of the specific heat divided by temperature for pure (closed circles) and Cd-doped (open circles) Ce_2RhIn_8 are plotted in Fig. 2(a). The Néel temperature obtained from the peak at the magnetic specific-heat data is in good agreement with the temperatures where the maximum in the magnetic susceptibility occurs (Fig. 1). We can observe the evolution of the Néel temperature from 2.8 K for pure sample to 4.8 K for Cd-doped sample showing that Cd-doping is enhanced the AFM character of this compound. The increasing of T_N as a function of Cd-doping was also found for Cd-doped $CeRhIn_5$ [9], which was interpreted to be a result of a local decrease of the electronic density of state that favors the antiferromagnetism. The fact the Cd-doping causes the same effect in Ce_2RhIn_8, which is also a heavy fermion antiferromagnet that becomes superconducting under pressure gives more support to the that argument.

The temperature dependence of the electrical resistivity for the doped compound is plotted in Fig. 2(b). The room-temperature value of the electrical resistivity is about $170\,\mu\Omega\,cm$ and the high-temperature data show a weak metallic behavior for this compound. Decreasing the temperature down to 150 K the resistivity increases reaching a maximum close to 10 K and then decreases at lower temperatures showing a clear kink around $T_N \approx 4.8\,K$ (inset of Fig. 2(b)). The residual resistivity of the single crystals of Cd-doped Ce_2RhIn_8 is roughly two orders of magnitude larger than the residual resistivity of the $CeMIn_5$ (M = Co, Rh, Ir) compounds. This behavior suggests a large disorder in the $2 - 1 - 8$ materials compared to that in the $1 - 1 - 5$.

The microscopic low-temperature magnetism of the Cd-doped Ce_2RhIn_8 with 20% of nominal concentration was further investigated by XRMS. Temperature-dependent magnetic peaks were observed in the dipolar resonant condition at temperatures below $T_N = 4.8\,K$ at reciprocal lattice points forbidden for charge scattering and consistent with an antiferromagnetic structure with propagation vector $(\frac{1}{2}, \frac{1}{2}, 0)$. This result is the same found by Wey et al. [17] for the pure compound, showing that Cd-doping is not changing the propagation vector. This indicates that although the Cd-doping enhances the magnitude of the average magnetic exchange between neighboring Ce^{3+} ions it does not affect the

a

b
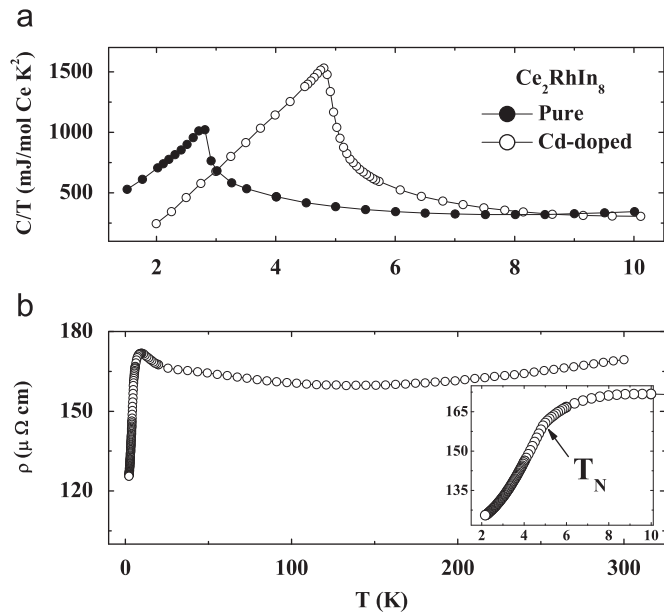
Fig. 2. (a) Specific-heat data divided by temperature as a function of temperature for pure (close circles) and Cd-doped (open circles) Ce_2RhIn_8. (b) Temperature dependence of the electrical resistivity for Cd-doped sample. The current has been applied parallel to the ab plane. The inset in (b) point out a kink at the Néel temperature for this compound.

sign of the relative magnetic interaction (and spin orientation) between them.

In the case of Cd-doped $CeCoIn_5$ [15], the magnetic structure was found to be commensurate with a propagation vector $(\frac{1}{2}, \frac{1}{2}, \frac{1}{2})$ in contrast to the incommensurate antiferromagnetic ordering $(\frac{1}{2}, \frac{1}{2}, \delta)$ observed in the related compound $CeRhIn_5$. However, in this case the comparison is not direct because $CeRhIn_5$ is a different compound and the pure $CeCoIn_5$ does not orders magnetically.

The energy line shape curve for the polarization channel $\sigma-\pi'$ of the $(\frac{1}{2}, \frac{1}{2}, 9)$ diffraction peak at the L_2 absorption edge of Ce at $T = 2$ K is shown in Fig. 3.

The energy scan curve in Fig. 3 has a maximum at 6.164 keV which is the value of the L_2 absorption edge of Ce, this behavior revealing the electric dipolar character ($E1$) of this transition (from $2p$ to $5d$ states). The polarization analysis were performed to unambiguously confirm the magnetic origin of the superstructure peaks. For the experimental configuration used (incident σ-polarization), $E1$ transitions rotate the plane of polarization into the scattering plane (π-polarization). Our data in Fig. 3 reveals a strong enhancement of the scattered intensities at the $\sigma-\pi'$ channel and no enhancement at the $\sigma-\sigma'$ channel (not showed) for the same energy range.

These results confirm the magnetic origin of the $(\frac{1}{2}, \frac{1}{2}, l)$ reflections due to the existence of an antiferromagnetic structure doubled in the basal plane. Fig. 4 shows the rocking curve obtained at $(\frac{1}{2}, \frac{1}{2}, 9)$ taken at 2 K in resonance mode at $\sigma-\pi'$ polarization channel. We performed the scan at the same position to the $\sigma-\sigma'$ polarization channel and no signal was observed. The peak of Fig. 4 was fitted using a squared Lorentzian curve showed in the graph (continuous line), the parameters obtained give us the integrated intensity and the full width half maximum (FWHM). The value of the FWHM was found to be 0.05˚ showing the good quality of the single crystal, and the integrated intensity can be used to determine the magnetic structure of the sample. Rocking scans at the $(\frac{1}{2}, \frac{1}{2}, l)$ direction were made to yield the study of the magnetic structure.
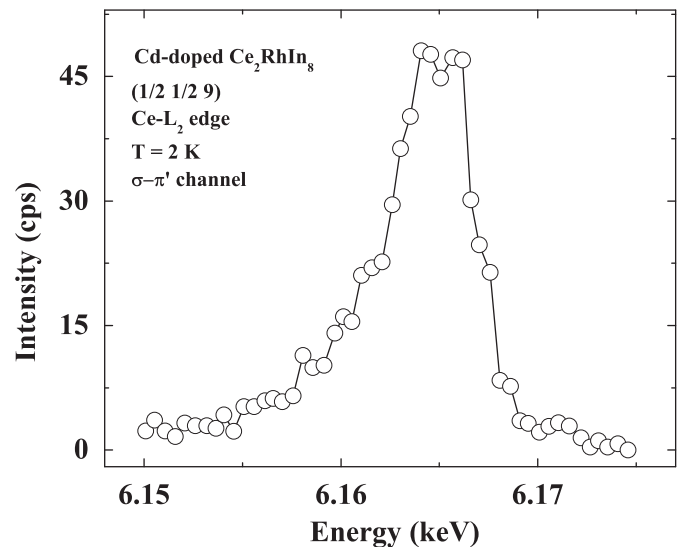
Fig. 3. Energy lineshape of the $(\frac{1}{2}, \frac{1}{2}, 9)$ magnetic peak at $T = 2$ K for $\sigma-\pi'$ polarization channel at the L_2 absorption edge of Ce. The line is just a guide to the eyes.
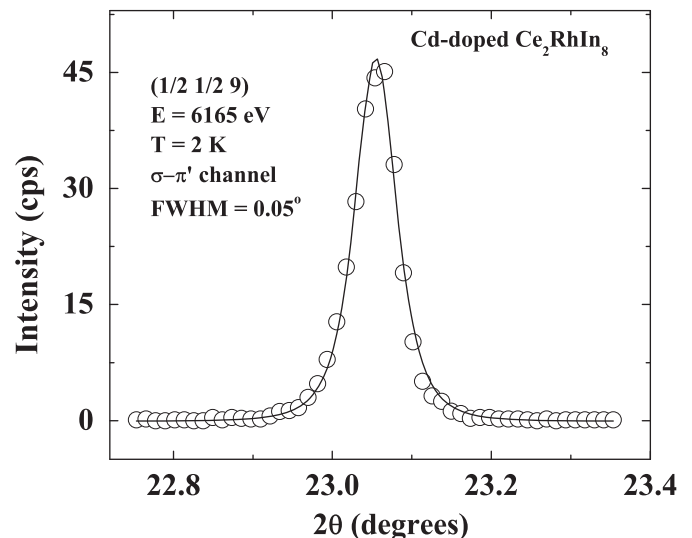
Fig. 4. Rocking scan through magnetic peak $(\frac{1}{2}, \frac{1}{2}, 9)$ at 2 K and 6164 eV for $\sigma-\pi'$ polarization channel at the L_2 absorption edge of Ce. The line is the best fit obtained with a squared Lorentzian curve.

Finally, an important piece of information regarding the determination of a magnetic structure is the orientation of the magnetic ordered moment with respect to the crystal lattice. While the magnetic wave vector gives the relative orientation between the neighboring spins, the direction of moment gives information about the magnetic anisotropy (e.g. CEF effects) of the ordered spins.

In principle, fits to the integrated intensities of all magnetic peaks can be used to determine the magnetic moment direction [23,26–29]. However, in some cases the number and intensity of the measured magnetic peaks is not enough to unambiguously determine the direction of moment. For instance, the direction of the magnetic moment for Cd-doped $CeCoIn_5$ were not resolved [15]. Careful and complete analysis of the magnetic peaks integrated intensity for Cd-doped Ce_2RhIn_8 are in progress and the definite conclusion will be published elsewhere along with further experiments in samples with different Cd-concentrations.

4. Conclusions

In summary, we report the physical properties of a Cd-doped Ce_2RhIn_8 sample with nominal concentration of 20% of Cd. The results of the susceptibility, heat-capacity and resistivity as a function of temperature revealed an enhancement of the Néel temperature from 2.8 K for pure compound to 4.8 K for Cd-doped sample. This result confirms the trend observed for the $1-1-5$ compounds that the Cd-doping favors the AFM ordering in these series. The XRMS experiments show that Cd-doped Ce_2RhIn_8 has a commensurate magnetic order with propagation vector $\vec{\eta} = (\frac{1}{2}, \frac{1}{2}, 0)$ similar to the pure compound, indicating that the Cd-doping does not alter the sign of the relative magnetic interaction between the neighboring Ce spins, although it increases the magnitude of the average magnetic interaction between them.

Acknowledgments

References

[1] See for instance: P. Monthoux, G.G. Lonzarich, Phys. Rev. B 59 (1999) 14598.
[2] T. Park, et al., Nature 440 (2006) 65.
[3] H. Hegger, C. Petrovic, E.G. Moshopoulou, M.F. Hundley, J.L. Sarrao, Z. Fisk, J.D. Thompson, Phys. Rev. Lett. 84 (2000) 4986.
[4] C. Petrovic, P.G. Pagliuso, M.F. Hundley, R. Movshovich, J.L. Sarrao, J.D. Thompson, Z. Fisk, P. Monthoux, J. Phys.: Condens. Matter 13 (2001) L337.
[5] P.G. Pagliuso, N. J Curro, N.O. Moreno, M.F. Hundley, J.D. Thompson, J.L. Sarrao, Z. Fisk, Phys. B 320 (2002) 370.
[6] P.G. Pagliuso, N.O. Moreno, N.J. Curro, J.D. Thompson, M.F. Hundley, J.L. Sarrao, Z. Fisk, Phys. Rev. B 66 (2002) 054433.
[7] P.G. Pagliuso, C. Petrovic, R. Movshovich, D. Hall, M.F. Hundley, J.L. Sarrao, J.D. Thompson, Z. Fisk, Phys. Rev. B 64 (2001) 100503(R).
[8] L. Mendonça-Ferreira, T. Park, V. Sidorov, M. Nicklas, E.M. Bittar, R. Lora-Serrano, E.N. Hering, S.M. Ramos, M.B. Fontes, E. Baggio-Saitovich, H. Lee, J.L. Sarrao, J.D. Thompson, P.G. Pagliuso, Phys. Rev. Lett. 101 (2008) 017005.
[9] L.D. Pham, T. Park, S. Maquilon, J.D. Thompson, Z. Fisk, Phys. Rev. Lett. 97 (2006) 056404.
[10] E.D. Bauer, et al., Phys. Rev. B 73 (2006) 245109.
[11] G.-q. Zheng, et al., Phys. Rev. B 70 (2004) 014511.
[12] W. Bao, A.D. Christianson, P.G. Pagliuso, J.L. Sarrao, J.D. Thompson, A.H. Lacerda, J.W. Lynn, Phys. B 312–313 (2002) 120.
[13] S.M. Ramos, M.B. Fontes, A.D. Alvarenga, E. Baggio-Saitovich, P.G. Pagliuso, E.D. Bauer, J.D. Thompson, J.L. Sarrao, M.A. Continentino, Physica B 359–361 (2005) 398.
[14] M. Daniel, et al., Phys. Rev. Lett. 95 (2005) 016406.
[15] M. Nicklas, O. Stockert, T. Park, K. Habicht, K. Kiefer, L.D. Pham, J.D. Thompson, Z. Fisk, F. Steglich, Phys. Rev. B 70 (2004) 014511.
[16] R.R. Urbano, B.-L. Young, N.J. Curro, J.D. Thompson, L.D. Pham, Z. Fisk, Phys. Rev. Lett. 99 (2007) 146402.
[17] W. Bao, P.G. Pagliuso, J.L. Sarrao, J.D. Thompson, Z. Fisk, Phys. Rev. B 64 (2001) 020401(R).
[18] N.O. Moreno, M.F. Hundley, P.G. Pagliuso, R. Movshovich, M. Nicklas, J.D. Thompson, J.L. Sarrao, Z. Fisk, Physica B 312–313 (2002) 274.
[19] P.G. Pagliuso, J.D. Thompson, M.F. Hundley, J.L. Sarrao, Z. Fisk, Phys. Rev. B 63 (2001) 054426.
[20] Z. Fisk, J.P. Remeika, Handbook on the Physics and Chemistry of Rare Earths, vol. 12, Elsevier, North-Holland, Amsterdam, 1989, p. 53.
[21] P.G. Pagliuso, J.D. Thompson, M.F. Hundley, J.L. Sarrao, Phys. Rev. B 62 (2000) 12266.
[22] P.G. Pagliuso, D.J. Garcia, E. Miranda, E. Granado, R. Lora Serrano, C. Giles, J.G.S. Duque, R.R. Urbano, C. Rettori, J.D. Thompson, M.F. Hundley, J.L. Sarrao, J. Appl. Phys. 99 (2006) 08P703.
[23] R. Lora-Serrano, C. Giles, E. Granado, D.J. Garcia, E. Miranda, O. Agüero, L. Mendonça Ferreira, J.G.S. Duque, P.G. Pagliuso, Phys. Rev. B 74 (2006) 214404.
[24] N.V. Hieua, H. Shishido, H. Nakashima, K. Sugiyama, R. Settai, T. Takeuchi, T.D. Matsuda, Y. Haga, M. Hagiwara, K. Kindo, Y. Onuki, J. Magn. Magn. Mater. 310 (2007) 1721.
[25] J. Hudis, R. Hu, C.L. Broholm, V.F. Mitrović, C. Petrovic, J. Magn. Magn. Mater. 307 (2006) 301.
[26] J.P. Hill, D.F. McMorrow, Acta Crystallogr. Sect. A Found. Crystallogr. A 52 (1996) 236.
[27] C. Adriano, R. Lora-Serrano, C. Giles, F. de Bergevin, J.C. Lang, G. Srajer, C. Mazzoli, L. Paolasini, P.G. Pagliuso, Phys. Rev. B 76 (2007) 104515.
[28] E. Granado, P.G. Pagliuso, C. Giles, R. Lora-Serrano, F. Yokaichiya, J.L. Sarrao, Phys. Rev. B 69 (2004) 144411.
[29] D. Mannix, P.C. de Camargo, C. Giles, A.J.A. de Oliveira, F. Yokaichiya, C. Vettier, Eur. Phys. J. B 20 (2001) 19–25.